An ATP-Linked Structural Change in Protein Kinase A Precedes Phosphoryl Transfer under Physiological Magnesium Concentrations†

Jennifer Shaffer and Joseph A. Adams*

Department of Chemistry, San Diego State University, San Diego, California 92182-1030

Received November 20, 1998; Revised Manuscript Received February 16, 1999

ABSTRACT: The kinetic mechanism for the catalytic subunit of protein kinase A was evaluated using physiological concentrations of free magnesium (0.5 mM) and a rapid quench flow technique. When the enzyme is pre-equilibrated with ATP, the peptide substrate, LRRASLG (Kemptide), is phosphorylated in a biphasic manner with a rapid, exponential "burst" phase (k_b) followed by a slower, linear phase (k_L) that corresponds to the steady-state kinetic rate. Both the amplitude and the substrate−rate dependence of the initial, burst phase indicate that the rate of phosphoryl transfer is fast (approximately 500 s^{-1}) and does not limit turnover (45 s^{-1}). Viscosity studies indicate that, while Kemptide is in rapid equilibrium, ATP does not exchange rapidly with the active site and k_{cat}/K_{ATP} is limited by the rate constant for nucleotide encounter. When the pre-steady-state kinetic experiments are initiated with ATP, a lag phase is observed at low ATP concentrations consistent with rate-limiting association. At high ATP concentrations (>1 mM), a burst phase is observed but the rate and amplitude are low on the basis of the bimolecular rate constant for ATP association and the rate constant for phosphoryl transfer. The kinetic data indicate that the phosphoryl transfer step is fast at physiological magnesium concentrations, but an ATP-linked conformational change precedes this step, limiting the burst phase rate constant. Simulations of the pre-steady-state kinetic transients indicate that turnover (45 s^{-1}) is limited both by net product release (70 s^{-1}) and by this structural change (170 s^{-1}). This structural change may also occur at high free magnesium concentrations, but it must be significantly faster than 170 s^{-1} and, consequently, not rate-limiting for turnover (k_{cat} = 20 s^{-1} at 10 mM free Mg^{2+}). We propose that this conformational event is an obligatory component of the kinetic pathway and includes a movement of the catalytic residues necessary for supporting phosphoryl group donation.

Protein kinase A [PKA][1] catalyzes the phosphorylation of numerous protein targets in response to the intracellular messenger, cAMP. This latter molecule binds tightly to the inactive, tetrameric form of the enzyme, releasing two active catalytic subunits (C) and a cAMP-bound regulatory dimer (R_2). The utilization of this enzyme in signal transduction pathways is widespread and can impact many cellular processes including lipid and carbohydrate metabolism, catecholamine biosynthesis, muscle contraction, and DNA transcription. PKA was the second protein kinase discovered but has become the paradigm for this family of enzymes for several reasons. First, active PKA can be readily obtained in large amounts either from tissue sources or in recombinant form (*2*). Second, the C-subunit of PKA is small (40 000 kDa) and contains no regulatory domains that influence activity. Third, PKA was the first protein kinase structure to be solved by X-ray diffraction methods and, since then, many forms of active PKA have now been solved with various nucleotides, divalent metal ions and inhibitor, substrate, and product peptides bound (*3*−*6*).

PKA requires an essential, high-affinity Mg^{2+} for catalysis. On the basis of this X-ray data, this metal chelates the β and γ phosphates of ATP and is held in position by a conserved aspartic acid residue, Asp-184 (*4*). In the absence of this metal, ATP binds poorly and no phosphoryl transfer is observed. When the concentration of Mg^{2+} exceeds that for ATP, a condition found in living cells (*7*), a second, lower-affinity site becomes occupied. This metal chelates the α and γ phosphates of ATP and is positioned by Asn-171 of the catalytic loop (*4*). This site has been termed the "inhibitory" site since its occupancy reduces turnover (k_{cat}) by approximately 5−6-fold (*8*). Although other protein kinases bind two metal ions, there is no common, functional role for the second metal. For instance, while the second metal reduces turnover in PKA, it enhances turnover and is essential for catalysis for two other tyrosine protein kinases, Csk and Src (*9*). Furthermore, this metal lowers the K_m for ATP in PKA and v-Fps, an oncogenic tyrosine protein kinase (*10*), but has no effect on this parameter for Csk and Src (*9*). Finally, the affinity of the second magnesium ion can vary significantly. For example, the dissociation constant for the second metal in PKA and v-Fps is 2 mM and less than 0.3 mM, respectively (*8*, *10*).

† This work was supported by NIH grant GM 54846 and by the California Metabolic Research Foundation.

* To whom correspondence should be addressed. Telephone: (619) 594−6196. Fax: (619) 594−1879. E-mail: jadams@sundown.sdsu.edu.

[1] Abbreviations: C-subunit, catalytic subunit of protein kinase A; Kemptide, peptide sequence LRRASLG; Mops, 3-[*N*-Morpholino] propanesulfonic acid; PKA, cAMP-dependent protein kinase.

10.1021/bi982768q CCC: $18.00
Published on Web 04/03/1999

It is not clear why protein kinases respond differently to free concentrations of magnesium, but the complex behavior of the steady-state kinetic parameters warrants further investigation into the role of metal ions in catalysis. In our laboratory, we used a rapid quench flow procedure to show that the phosphoryl transfer step in PKA is 25-fold faster than k_{cat} (*1*). This demonstrates decisively that phosphoryl transfer does not limit k_{cat}, but, under conditions of low substrate concentration (i.e., V/K conditions), catalysis is limited by the ratio of phosphoryl transfer and the dissociation constant for the substrate (k_3/K_d). While stopped-flow kinetic analyses of a fluorescently labeled PKA mutant provided support for a viscosity-sensitive conformational change which partially limits turnover (*11*), no evidence for such a step was found in the wild-type enzyme at high magnesium concentration (*12*). These rapid mixing studies are useful for understanding the function of PKA but were performed under nonphysiological concentrations of 10 mM free Mg^{2+} when more than 80% of the second site is occupied. To gain insight into the rate of phosphoryl transfer and to establish a complete kinetic mechanism for PKA under cellular magnesium levels, we performed pre-steady-state kinetic studies at 0.5 mM free Mg^{2+} and compared them to those previously reported at 10 mM Mg^{2+} (*1*). The data show that the phosphoryl transfer step is fast and does not limit turnover at both concentrations of magnesium. However, a detailed analysis of the dependence of substrate and ATP concentrations on the pre-steady-state kinetic transients provides evidence that an ATP-linked conformational change precedes phosphoryl transfer and partially limits turnover.

MATERIALS AND METHODS

Materials. Adenosine triphosphate (ATP), 3-(*N*-morpholino) propane sulfonic acid (Mops), lactate dehydrogenase, pyruvate kinase, nicotinamide adenine dinucleotide, reduced (NADH), and phosphoenolpyruvate were purchased from Sigma Chemicals. Magnesium chloride, phosphoric acid, and liquid scintillant were obtained from Fisher Scientific. Phosphocellulose filter disks were purchased from Whatman, and [γ-^{32}P] ATP was obtained from NEN Products.

Peptide and Enzyme. The heptameric peptide, LRRASLG (Kemptide), was synthesized at the USC Microchemical Core Facility using Fmoc chemistry and purified by C-18 reverse-phase HPLC. The inhibitor peptides, LRRNALG and LRRAALG, were provided to us by Susan Taylor and Siv Garrod. Kemptide concentrations were determined by turnover with the C-subunit under conditions of limiting peptide in the spectrophotometric assay. Recombinant C-subunit was expressed in *Escherichia coli* and purified according to previously published procedures (Yonemoto et al.). The concentration of the enzyme was measured by its absorbance at 280 nm ($A_{0.1\%} = 1.2$).

Coupled Enzyme Assay. The enzymatic activity of the C-subunit was determined as described previously (Cook et. al., 1982). The oxidation of NADH, monitored spectrophotometrically as an absorbance decrease at 340 nm, is coupled to the production of ADP by lactate dehydrogenase and pyruvate kinase. All reactions were measured in a Beckman DU640 spectrophotometer equipped with a microcuvette holder. Typical steady-state kinetic assays were performed in 50 mM Mops (pH 7) in a final volume of 60 μL at 24 °C. PKA (6−60 nM) was typically incubated with 0.1−5 mM ATP, varying free magnesium (0.5−10 mM), 1 mM phosphoenolpyruvate, 0.3 mM NADH, 12 units of lactate dehydrogenase, and 4 units of pyruvate kinase for several minutes before initiating the reaction with peptide. Background reactions were recorded in the absence of Kemptide (ATPase activity) but were never more than 3% of the Kemptide-dependent reaction over all substrate concentrations. The total concentration of $MgCl_2$ needed to obtain a desired free concentration of Mg^{2+} was calculated on the basis of the dissociation constants of 0.0143 mM for Mg-ATP, 5 mM for Mg−PEP, and 19.5 mM for Mg−NADH (*13*).

Rapid Quench Flow Measurements. Pre-steady-state kinetic measurements were made using a KinTek Corporation Quench Flow Apparatus Model RGF-3 and a previously published procedure (*1*). Quench flow experiments were typically executed by loading equal volumes of enzyme, buffer, magnesium chloride, and [γ-^{32}P] ATP (600−2000 cpm pmol^{-1}) into one sample loop and Kemptide and magnesium chloride into the other in 50 mM Mops (pH 7). Variations on this mixing scheme are stated in the text. The reactions were quenched using 30% acetic acid, and phosphorylated Kemptide was separated from unreacted ATP by a filter binding assay (*14*). A portion of each quenched reaction (55 μL) was spotted onto a phosphocellulose filter disk and was washed four times with 0.5% phosphoric acid. The filter disks were rinsed with acetone, dried, and counted on the ^{32}P channel in liquid scintillant. Control experiments were performed to determine the background phosphorylation (i.e., phosphorylation of peptide in the presence of quench) and phosphokemptide retention on washed filter disks using previously published protocols (*1*). The time-dependent concentration of phosphokemptide was then determined by considering the total counts per minute (CPM) on each disk, the specific activity of the [^{32}P-γ] ATP label, the total collected volume, the background phosphorylation, and the phosphokemptide retention on washed filter disks.

Viscosometric Measurements. The relative solution viscosities (η^{rel}) of buffers containing glycerol were measured relative to a standard buffer of 50 mM Mops, pH 7.0, at 24 °C, using an Ostwald viscometer (*15*). Each viscosity measurement was carried out using 5.0 mL of buffer containing varying amounts of viscosogen, glycerol. The following relative solvent viscosities were obtained for the buffers (% viscosogen, η^{rel}): 35% glycerol, 2.9; 30% glycerol, 2.4; 20% glycerol, 1.9; 15% glycerol, 1.5.

Data Analysis. Data in the quench flow time courses were fit to an empirical function containing a single exponential and a linear component:

$$y = \alpha[E]_t[1 - \exp(-k_b t)] + Lt \quad (1)$$

where y is the concentration of phosphopeptide, α is the observed burst amplitude, k_b is the observed burst rate constant, and L is the observed linear rate. The observed linear rate constant, k_L, can be determined from the ratio of L and the enzyme concentration ($k_L = L/[E]_o$). Plots of the observed values for k_L were fit to the Michaelis−Menten equation to obtain k_{cat}, $K_{peptide}$, and K_{ATP}. Plots of α either as a function of ATP concentration (fixed Kemptide concentra-

Table 1: Steady-State Kinetic Parameters for Kemptide Phosphorylation at 0.5 and 10 mM Free Mg^{2+} [a]

parameter	[Mg^{2+}] free (mM) 0.5	10
k_{cat} (s^{-1})	45 ± 5.0	22[b]
$K_{peptide}$ (μM)	8.3 ± 4.1	6.9[b]
K_{ATP} (μM)	200 ± 20	17[c]
k_{cat}/K_{ATP} (μM^{-1} s^{-1})	0.22 ± 0.033	1.3
$k_{cat}/K_{peptide}$ (μM^{-1} s^{-1})	5.4 ± 2.7	3.2[b]
K_I (LRRAALG) (μM)[d]	40 ± 8	190[b]
K_I (LRRNALG) (μM)[d]	20 ± 6	

[a] The kinetic parameters were measured using the coupled enzyme assay in 50 mM Mops (pH 7). [b] These data were taken from ref *1*. [c] These data were taken from ref *11*. [d] C-subunit (16 nM) was pre-equilibrated with 2 mM ATP, 2.5 mM $MgCl_2$, and varying inhibitor (0.05−0.4 mM), and the reaction was initiated with Kemptide (200 μM for LRRNALG and 66 μM for LRRAALG). The initial velocity of the reaction was plotted as a function of inhibitor concentration, and the data were fit to the Michaelis−Menten equation where the apparent $K_{peptide}$ ($^{app}K_{peptide}$) is given by the following relationship: $^{app}K_{peptide} = K_{peptide}(1 + [I]/K_I)$.

tion) or as a function of Kemptide concentration (fixed ATP concentration) were fit to eq 2:

$$y = \left[\frac{\alpha_{max}/[E]_o[S]}{[S] + K_{app}}\right]^n \quad (2)$$

where y is the normalized amplitude ($\alpha/[E]_o$) at any given Kemptide or ATP concentration, $\alpha_{max}/[E]_o$ is the maximal, normalized amplitude, and K_{app} is the concentration at which 50% of $\alpha_{max}/[E]_o$ is achieved. The value of n is 1 for plots of $\alpha/[E]_o$ versus ATP concentration and the value of n is 2 for plots of $\alpha/[E]_o$ versus Kemptide concentration. The data were fit using the Macintosh computer graphics program, Kaleidagraph (Synergy Software), which utilizes an iterative least-squares algorithm. Some pre-steady-state kinetic data were similated using the numerical integration program KINSIM (*16*).

RESULTS

Steady-State Kinetic Parameters and Inhibition Constants for PKA. The steady-state kinetic parameters for the C-subunit of PKA at fixed, free magnesium (0.5 mM) were measured. The K_m for peptide ($K_{peptide}$) was measured from a plot of initial velocity versus Kemptide (8−800 μM) at fixed ATP (2 mM) and $MgCl_2$ (2.5 mM). The K_m for ATP (K_{ATP}) was measured from a plot of initial velocity versus ATP (0.05−1.5 mM) at fixed Kemptide (1 mM) and free Mg^{2+} (0.5 mM). From these plots, k_{cat}, $K_{peptide}$, and K_{ATP} were measured and are listed in Table 1. These values for the recombinant mouse enzyme are consistent with previously reported parameters using bovine PKA at 0.5 mM free Mg^{2+} (*8*). The steady-state kinetic parameters for recombinant mouse PKA at 10 mM free magnesium are included in Table 1 for comparison. While free magnesium does not affect $K_{peptide}$, the values for k_{cat} and K_{ATP} are 2- and 12-fold higher at low compared to high free metal. The 2-fold inhibitory effect of high magnesium on k_{cat} is offset by a lower K_{ATP} so that k_{cat}/K_{ATP} is actually 6-fold higher.

The steady-state turnover rate constant for the C-subunit of PKA was measured as a function of free Mg^{2+}. A plot of k_{cat} versus free Mg^{2+} is shown in Figure 1. Fitting the data

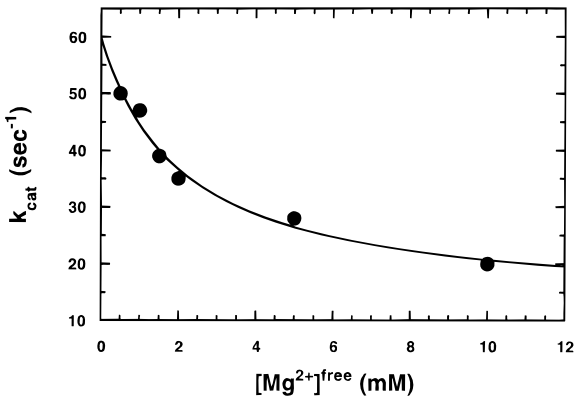

FIGURE 1: Turnover rate constant (k_{cat}) for the phosphorylation of Kemptide as a function of free Mg^{2+}. C-subunit (7.2 nM) was pre-equilibrated with ATP (5 mM) and varying, free Mg^{2+} (0.5−10 mM), and the reaction was initiated with 400 μM Kemptide in 50 mM Mops, pH 7. The total concentration of $MgCl_2$ ranged from 5.4 to 15 mM. The initial velocity of the reaction was monitored using the coupled enzyme assay, and k_{cat} was measured from the ratio of the initial velocity and the total enzyme concentration.

to a hyperbolic function provides observed rate constants at 0 ($^{\circ}k_{cat}$) and infinite ($^{max}k_{cat}$) free Mg^{2+} of 60 ± 10 and 12 ± 4 s^{-1}, respectively. The concentration of free magnesium at which the half-maximal rate is achieved (K_{Mg}) is 2.1 ± 0.50 mM. These values for the recombinant mouse PKA are consistent with those previously reported for the bovine enzyme (*8*). The observed affinity for magnesium implies that the second metal site is approximately 80% and 20% occupied at 10 and 0.5 mM free Mg^{2+}, respectively. Finally, the inhibitory constants (K_I) for two competitive inhibitors, LRRNALG and LRRAALG, were determined at 0.5 mM free Mg^{2+} using the coupled enzyme assay. The K_I values for LRRNALG and LRRAALG are reported in Table 1 and are between 2- and 5-fold larger than $K_{peptide}$.

Effects of Solvent Viscosity on the Steady-State Kinetic Parameters. The effects of solvent viscosity on the phosphorylation of LRRASLG were measured using the coupled enzyme assay. The ratios of k_{cat} and k_{cat}/K_{ATP} in the absence and presence of glycerol [$(k_{cat})^{\circ}/(k_{cat})$ or $(k_{cat}/K_{ATP})^{\circ}/(k_{cat}/K_{ATP})$] are plotted in Figure 2 as a function of relative solvent viscosity (η^{rel}). The data are fit to linear functions, and the slope values [$(k_{cat})^{\eta}$ or $(k_{cat}/K_{ATP})^{\eta}$] are included in Table 2. An accurate determination of the effects of solvent viscosity on $k_{cat}/K_{peptide}$ was not possible using the coupled enzyme assay owing to the low value of $K_{peptide}$ and the large error associated with its measurement (Table 1). To circumvent this problem, we measured an apparent $k_{cat}/K_{peptide}$ ($^{app}k_{cat}/K_{peptide}$) in the presence of a competitive inhibitor (*1*). This inhibitor, LRRNALG, increases the observed $K_{peptide}$ without affecting k_{cat} (*17*). The values of $^{app}k_{cat}/K_{peptide}$ were determined from linear fits of the plots of velocity versus Kemptide concentration. At 0% glycerol, $^{app}k_{cat}/K_{peptide}$ is 50 mM^{-1} s^{-1}, a value consistent with the K_I for LRRNALG (Table 1). The values of $^{app}k_{cat}/K_{peptide}$ in the absence and presence of glycerol [$(^{app}k_{cat}/K_{peptide})^{\circ}/(^{app}k_{cat}/K_{peptide})$] as a function of relative solvent viscosity (η^{rel}) are shown in Figure 2. No changes in this parameter were measured at the highest glycerol concentrations, indicating that $(^{app}k_{cat}/K_{peptide})^{\eta}$ is close to 0 (Table 2). Finally, we have shown previously that the K_I for LRRAALG is similar at 0% and 30% glycerol (*1*), indicating that the lack of a viscosity effect

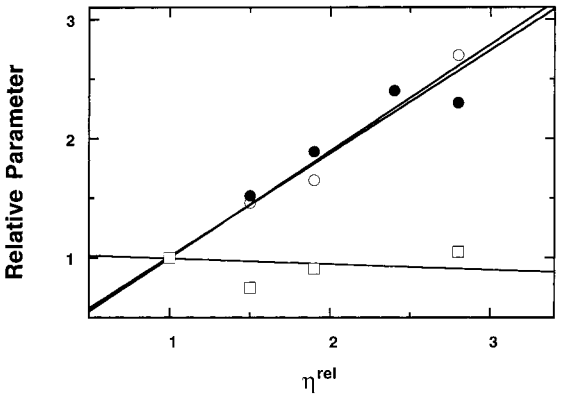

FIGURE 2: Effects of solvent viscosity on the steady-state kinetic parameters at 0.5 free Mg^{2+}. The kinetic parameters, k_{cat} (●), k_{cat}/K_{ATP} (○), and $^{app}k_{cat}/K_{peptide}$ (□), are plotted as relative values in the absence and presence of varying glycerol as a function of relative solvent viscosity (η^{rel}). The parameters, k_{cat} and k_{cat}/K_{ATP}, were measured using 200 μM LRRASLG, varying ATP (0.1−1 mM) and $MgCl_2$ (0.6−1.5 mM), and $^{app}k_{cat}/K_{peptide}$ was measured using varying Kemptide (50−200 μM), 2 mM ATP, and 2.5 mM $MgCl_2$ in the presence of 1 mM LRRNALG. All reactions were initiated with Kemptide. The data are fit with linear functions, and the slope values are listed in Table 2.

Table 2: Viscosity Effects on the Steady-State Kinetic Parameters for Kemptide Phosphorylation at 0.5 mM Free Mg^{2+} [a]

	[Mg^{2+}] free (mM)	
parameter	0.5	10
$(k_{cat})^{\eta}$	0.92 ± 0.04	1.0[b]
$(k_{cat}/K_{peptide})^{\eta}$	−0.04 ± 0.04	0[b]
$(k_{cat}/K_{ATP})^{\eta}$	0.90 ± 0.05	1.0[c]
k_1 (μM^{-1} s^{-1})[d]	0.24 ± 0.038	1.3
k_3 (s^{-1})[d]	560 ± 290	>220[b]
k_4 (s^{-1})[d]	49 ± 5.8	22[b]

[a] The kinetic parameters were measured using the coupled enzyme assay in 50 mM Mops (pH 7). [b] These data were taken from ref *1*. [c] This value is taken from ref *28*. [d] These rate constants were determined from the following relationships: $k_1 = k_{cat}/K_{ATP}/(k_{cat}/K_{ATP})^{\eta}$, $k_3 = k_{cat}/[1-(k_{cat})^{\eta}]$, $k_4 = k_{cat}/(k_{cat})^{\eta}$ (*28*).

on $k_{cat}/K_{peptide}$ is not due to a compensating effect on peptide affinity.

Pre-Steady-State Kinetics Using Variable ATP (E·ATP + S →). The phosphorylation of Kemptide on the millisecond time frame was measured using a rapid quench flow instrument and a radiochemical assay. Figure 3A shows pre-steady-state kinetic transients at fixed enzyme and Kemptide concentrations and two concentrations of ATP. In this experiment, C-subunit and ATP are pre-equilibrated prior to the addition of Kemptide. Under both concentrations of ATP, the kinetic transients are biphasic with a rapid, exponential (burst) phase followed by a slower, linear phase. The data are fit to eq 1 to obtain values for α and L of 1.4 ± 0.10 μM and 53 ± 3 μM/s at 0.2 mM ATP and 2.8 ± 0.21 μM and 145 ± 6 μM/s at 1.0 mM ATP, respectively. At both ATP concentrations, the burst rate constant, k_b, is approximately 500 s^{-1}.

Since the linear and exponential phases in Figure 3A are different at 0.2 and 1.0 mM ATP, the kinetics were performed at a series of ATP concentrations (0.1−2.0 mM) at fixed concentrations of Kemptide (0.2 mM). Figure 3B shows the effects of ATP concentration on the amplitude and linear phases of the pre-steady-state kinetic transients.

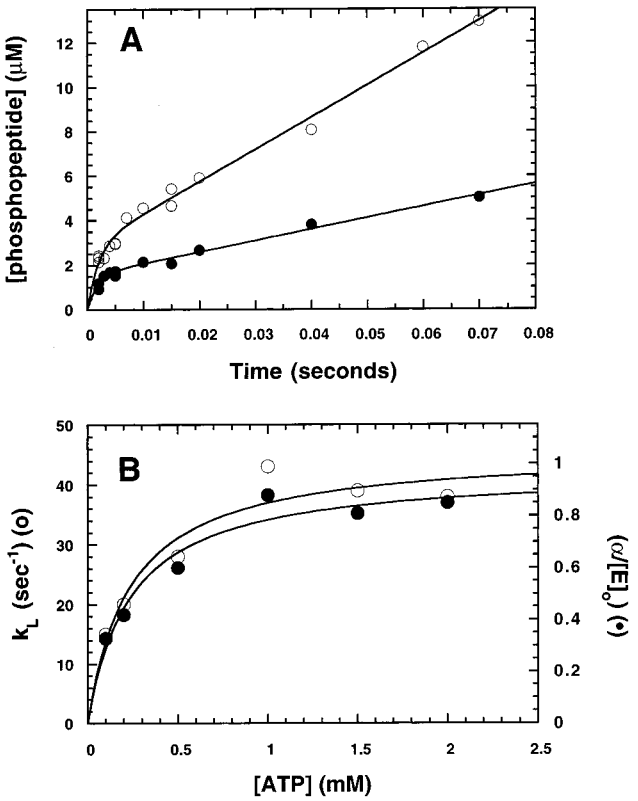

FIGURE 3: Phosphorylation of Kemptide using varied ATP (pre-equilibration with PKA) and fixed Kemptide at 0.5 mM free Mg^{2+}. (A) Production of phosphopeptide as a function of time at 1.0 (○) and 0.2 mM (●) ATP and 0.5 mM free Mg^{2+}. C-subunit (final concentration: 3.2 μM) is pre-equilibrated with ATP and Mg^{2+} prior to starting the reaction with 200 μM Kemptide in 50 mM Mops (pH 7). With the use of eq 1, the values of α and L are 1.4 ± 0.11 μM and 53 ± 5 μM/s at 0.2 μM and 2.8 ± 0.21 μM and 145 ± 6 μM/s at 1 mM ATP, respectively. At both ATP concentrations, k_b is approximately 500 s^{-1}. (B) Effects of ATP concentration on the amplitude (●) and linear (○) terms in the pre-steady-state kinetic transients. Each parameter was obtained from fitting the kinetic data to eq 1 using 0.1−2 mM ATP, 0.5 mM free Mg^{2+}, and 200 μM Kemptide. The normalized amplitude, $\alpha/[E]_o$, and the linear rate constant, k_L, were fit using eq 2 when $n = 1$ and the Michaelis−Menten equation. The parameter fits are listed in Table 3.

Table 3: Parameter Fits for the Pre-Steady-State Kinetic Transients When PKA Is Pre-equilibrated with ATP[a]

variable ligand	$\alpha_{max}/[E]_o$	K_{app} (μM)	k_{cat} (s^{-1})	K_m (μM)
ATP	0.95 ± 0.06	230 ± 77	46 ± 5	220 ± 80
Kemptide	0.86 ± 0.06	5.0 ± 2.9	44 ± 2	10 ± 3

[a] The kinetic parameters were measured using a radiochemical assay in 50 mM Mops, pH 7. The parameter fits originate from the data in Figures 3A and 4A using eq 2 for $\alpha_{max}/[E]_o$ and K_{app} ($n = 1$ for ATP as the variable ligand and $n = 2$ for Kemptide as the variable ligand) and the Michaelis−Menten equation for k_{cat} and K_m.

Both the normalized amplitude ($\alpha/[E]_o$) and the linear rate constant ($k_L = L/[E]_o$) vary hyperbolically with the nucleotide concentration at fixed Kemptide. The parameter fits are listed in Table 3. At all ATP concentrations, the burst rate constant (k_b) was approximately 500 s^{-1}. Given the deadtime of the rapid quench flow instrument (2 ms) and the fast, linear rate (46 s^{-1} at high ATP concentrations), it is difficult to assign accurately the rate of the burst phase, but on the basis of the high amplitude ($\alpha_{max}/[E]_o \cong 1$), we presume that the computer-generated value of k_b is a lower limit.[2]

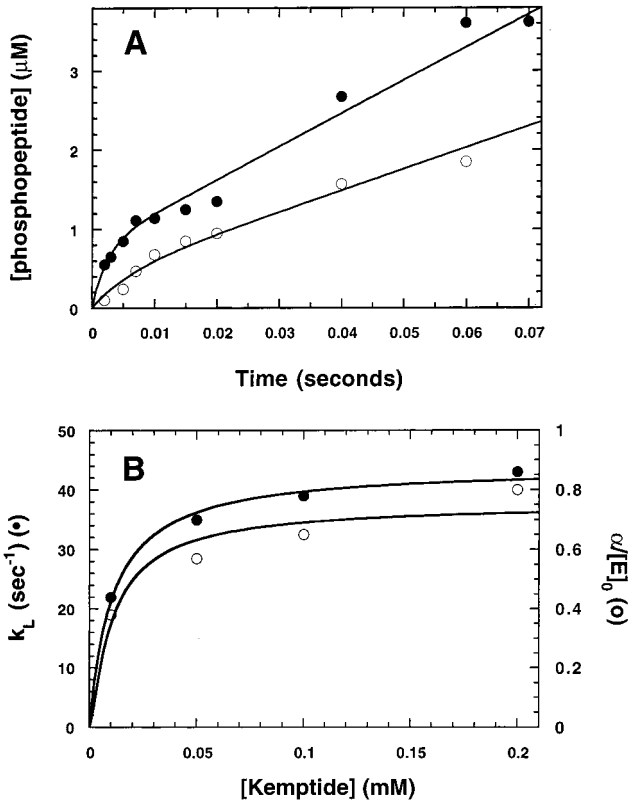

FIGURE 4: Phosphorylation of Kemptide using fixed ATP (pre-equilibrated with PKA) and variable Kemptide at 0.5 mM free Mg^{2+}. (A) Production of phosphopeptide as a function of time at 0.20 (●) and 0.010 mM (○) Kemptide. C-subunit (final concentration: 1 μM) is pre-equilibrated with ATP (final concentration: 1 mM) and 0.5 mM free Mg^{2+} prior to starting the reaction with varying Kemptide in 50 mM Mops, pH 7. Fitting of the two data sets to eq 1 gave values of 410 ± 180 s^{-1}, 0.80 ± 0.07 μM, and 43 ± 4 μM/s for k_b, α, and L, respectively, at 0.2 mM Kemptide. Values of 150 ± 30 s^{-1}, 0.39 ± 0.10 μM, and 22 ± 4 μM/s were obtained for k_b, α, and L, respectively, at 0.01 mM Kemptide. (B) Effects of Kemptide concentration on the amplitude (○) and the linear (●) terms in the pre-steady-state kinetic traces. Each parameter was obtained from fitting the kinetic data to eq 1 using 1 mM ATP, 0.5 mM free Mg^{2+}, and 10−200 μM Kemptide. The normalized amplitude, α/[E]$_o$, was fit to eq 2 when $n = 2$ and the linear rate constant, k_L, was fit using the Michaelis−Menten equation. The parameter fits are listed in Table 3.

Pre-Steady-State Kinetics Using Variable Kemptide (E·ATP + S →). To provide more information on the association of the peptide substrate with the enzyme, we measured the pre-steady-state kinetic transients using variable concentrations of Kemptide. In this experiment, C-subunit is pre-equilibrated with ATP and $MgCl_2$ and the reaction is started with varying amounts of Kemptide at 0.5 mM free Mg^{2+}. Figure 4A shows the production of phosphopeptide as a function of time at two concentrations of Kemptide (0.01 and 0.2 mM). Fitting of the two data sets to eq 1 gave values of 410 ± 180 s^{-1}, 0.80 ± 0.07 μM, and 42 ± 4 μM/s for k_b, α, and L, respectively, at 0.2 mM Kemptide. Values of 150 ± 30 s^{-1}, 0.39 ± 0.10 μM, and 23 ± 4 μM/s were obtained for k_b, α, and L, respectively, at 0.01 mM Kemptide. The values for k_L (L/[E]) of 23 and 42 s^{-1} at 0.01 and 0.2 mM Kemptide are consistent with the steady-state kinetic parameters in Table 1.

Since the kinetic transients in Figure 4A are different, rapid quench flow studies were performed at several concentrations of Kemptide. Experiments were performed as shown in Figure 4A except that the final concentration of Kemptide was varied from 0.01 to 0.20 mM. Under all conditions, the production of phosphopeptide followed biphasic kinetics (data not shown) and the data were fit using eq 1. Figure 4B shows the effects of Kemptide concentration on α/[E]$_o$ and k_L. The linear rate data were fit to the Michaelis−Menten equation to obtain values of 44 ± 2 s^{-1} and 10 ± 3 μM for k_{cat} and $K_{peptide}$. These values are consistent with the steady-state kinetic parameters obtained from the coupled enzyme assay (Table 1), verifying that the linear phase in Figure 3A measures the steady-state rate. The amplitude data were fit to eq 2 where $n = 2$ to obtain values of 0.86 ± 0.06 and 5.0 ± 2.9 μM for α_{max}/[E]$_o$ and K_{app} (Table 3). We have shown in a previous study that the burst amplitude varies as a squared function of the Kemptide concentration (eq 2 where $n = 2$) if the peptide rapidly exchanges with the active site (*1*). Under these conditions, which have been verified by the viscosity studies (Table 2), K_{app} is equal to $K_{peptide}$ (compare $K_{peptide}$= 8.3 μM and K_{app} = 5 μM; Tables 1 and 3). Between 50 and 200 μM Kemptide, k_b was fit to values of approximately 400 s^{-1} (data not shown). Given the deadtime of the rapid quench flow instrument (2 ms) and the fast, linear rate (k_L = 46 s^{-1}), it is difficult to assign accurately the rate of the burst phase in this concentration range. At 10 μM Kemptide, however, the observed burst rate was much slower (k_b = 150 s^{-1}).

Pre-Steady-State Kinetics Using Variable ATP (E + ATP/S →). To derive information on ATP binding at physiological magnesium concentrations, we performed the pre-steady-state kinetic experiments under conditions where PKA was not pre-equilibrated with ATP. Figure 5A shows the production of phosphopeptide (normalized to the enzyme concentration) as a function of time when PKA is mixed with Kemptide and two concentrations of ATP (0.2 and 3 mM). These experiments were repeated under identical conditions except Kemptide was pre-equilibrated with PKA and the reaction was initiated with ATP. No change in the time-dependent production of phosphopeptide was detected under these conditions (data not shown). The lines drawn through the data were generated from the kinetic simulation program KINSIM and Scheme 3 (see Discussion section). These experiments were also performed at 1, 2, and 4 mM ATP (data not shown).

Pre-Steady-State Kinetics Using 10 mM Free Magnesium. The original pre-steady-state experiments on PKA were performed with ATP and the enzyme pre-equilibrated before reaction initiation with Kemptide (*1*). Under these conditions, no direct information on ATP binding could be obtained. To expand our understanding of ATP association, we measured the phosphorylation of Kemptide using 0.5 and 10 mM free Mg^{2+} in the absence of ATP pre-equilibration. In this experiment, C-subunit and Kemptide are pre-equilibrated. The time-dependent production of phosphokemptide at both concentrations of free magnesium are shown plotted in Figure 6. The line drawn though the data at 10 mM free Mg^{2+} was generated using eq 1, and the line

[2] When the concentrations of ATP and Kemptide are high, the normalized amplitude of the "burst" phase (α_{max}/[E]$_o$) can be related to the rate of the phosphoryl transfer step (k_3) and the net rate for product release (k_4) by the following relationship: $\alpha_{max}/[E]_o = (k_3/(k_3 + k_4))^2$ (*1*). If $\alpha_{max}/[E]_o$ is close to 1, $k_3 \gg k_4$.

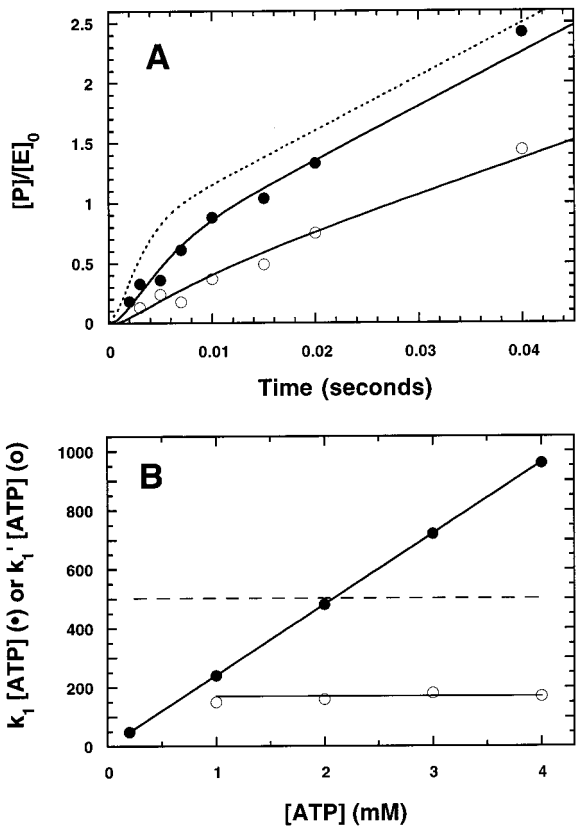

FIGURE 5: Phosphorylation of Kemptide using fixed Kemptide and variable ATP without pre-equilibration at 0.5 mM free Mg^{2+}. (A) Normalized production of phosphopeptide ($[P]/[E]_o$) as a function of time at 0.2 mM (○) and 3 mM (●) ATP. At 0.2 mM ATP, the final concentrations of PKA, Kemptide, and $MgCl_2$ are 2.4 μM, 200 μM, and 0.69 mM, respectively. At 3 mM ATP, the final concentrations of PKA, Kemptide, and $MgCl_2$ are 5.5 μM, 200 μM, and 3.42 mM, respectively. The lines drawn through the data were obtained from simulated data using Scheme 3 (see text). (B) Plot of k_1[ATP] (●) and k_1'[ATP] (○) as a function of ATP concentration. k_1 was determined from viscosity measurements (Table 2), and k_1' was determined from simulated data. The dashed line indicates the rate of phosphoryl transfer measured under conditions of ATP pre-equilibration.

drawn though the data at 0.5 mM free Mg^{2+} was generated from Scheme 3 using numerical integration (see text).

DISCUSSION

PKA requires an essential magnesium ion for catalysis but will bind a second metal which prominently influences substrate phosphorylation. In recombinant mouse PKA, complete occupancy of the second metal site lowers k_{cat} by 6-fold (Figure 1). By comparison, lowering the occupancy of the second site from 80% at 10 mM to 20% at 0.5 mM free Mg^{2+} decreases k_{cat}/K_{ATP} by 6-fold (Table 1). These large and opposing effects underscore the need for detailed kinetic analyses at physiological (0.5 mM) as well as high magnesium concentrations. We have shown previously that the rate of phosphoryl transfer is fast and does not limit turnover at 10 mM free Mg^{2+} (*1*). However, the selection of high, free concentrations of magnesium for kinetic assays does not adequately mimic the cellular environment which consists of approximately 0.5 mM free Mg^{2+} (*7*). With the recent progress in the X-ray analysis of protein kinases, it is now apparent that catalysis will be linked to subtle and large structure changes in and around the active site (*18*−*23*). It

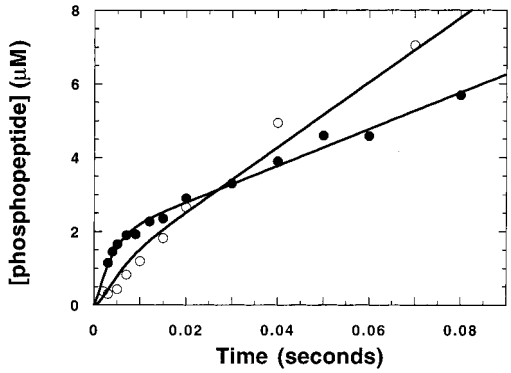

FIGURE 6: Phosphorylation of Kemptide using 0.5 mM (○) and 10 mM (●) free Mg^{2+} without ATP pre-equilibration. C-subunit (final concentration: 2 μM) is pre-equilibrated with Kemptide (final concentration: 200 μM), and the reaction is initiated with ATP (final concentration: 1 mM) in 50 mM Mops, pH 7. The final concentration of $MgCl_2$ is 11 mM. The line drawn through the data at 10 mM free Mg^{2+} was generated using eq 1: $k_b = 300 \pm 60$ s^{-1}, $\alpha = 1.8 \pm 0.11$ μM, and $k_L/[E] = 24 \pm 2$ s^{-1}. The line drawn through the data at 0.5 mM free Mg^{2+} was obtained from kinetic simulations using Scheme 3 (see text).

Scheme 1

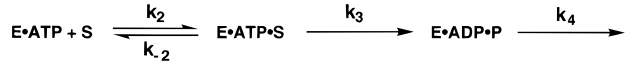

Scheme 2

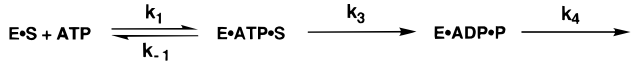

is, therefore, important to understand the delicate interplay between structural changes and catalytic mechanism. To address the role of low magnesium levels in controlling the phosphoryl transfer step and associated ligand binding and conformational steps, we measured the pre-steady-state kinetics of this enzyme at 0.5 mM free Mg^{2+} using a rapid quench flow technique.

Exchange Rates for ATP and Kemptide. To interpret the effects of free magnesium on Kemptide phosphorylation, we measured the influence of viscosogens on the steady-state kinetic parameters. Changes in the relative viscosity of the buffer have large effects on two parameters, k_{cat} and k_{cat}/K_{ATP}, without affecting $k_{cat}/K_{peptide}$ (Figure 2 and Table 2). We interpret these effects using the kinetic mechanisms in Schemes 1 and 2, where k_1 and k_{-1} are the association and dissociation rate constants for ATP, k_2 and k_{-2} are the association and dissociation rate constants for Kemptide, k_3 is the phosphoryl transfer rate constant, and k_4 is the net dissociation rate constant for the products. The rate constants for the individual steps in Schemes 1 and 2 can be derived on the basis of the sensitivity of k_{cat}, $k_{cat}/K_{peptide}$, and k_{cat}/K_{ATP} to added viscosogens using the Stokes−Einstein equation and the following relationships:

$$(k_{cat})^{\eta} = \frac{k_3}{k_3 + k_4} \quad (3)$$

$$(k_{cat}/K_{peptide})^{\eta} = \frac{k_3}{k_{-2} + k_3} \quad (4)$$

$$(k_{cat}/K_{ATP})^{\eta} = \frac{k_3}{k_{-1} + k_3} \quad (5)$$

where $(k_{cat})^{\eta}$, $(k_{cat}/K_{peptide})^{\eta}$, and $(k_{cat}/K_{ATP})^{\eta}$ are the slopes for the plots of $(k_{cat})^{\circ}/k_{cat}$, $(k_{cat}/K_{peptide})^{\circ}/(k_{cat}/K_{peptide})$, and $(k_{cat}/K_{ATP})^{\circ}/(k_{cat}/K_{ATP})$ versus η^{rel}, respectively. We can use the rate expressions for k_{cat} $[k_3k_4/(k_3+k_4)]$, $k_{cat}/K_{peptide}$ $[k_2k_3/(k_{-2}+k_3)]$, and k_{cat}/K_{ATP} $[k_1k_3/(k_{-1}+k_3)]$ and eqs 3−5 to determine or put limits on the individual steps in Schemes 1 and 2. These values, reported in Table 2, indicate that k_3 is fast and does not limit k_{cat}. However, on the basis of the value of $(k_{cat})^{\eta}$ there is a large uncertainty in the measurement of k_3. The absence of a viscosity effect on $(k_{cat}/K_{peptide})^{\eta}$ implies that Kemptide dissociates from the ternary complex, E·ATP·S, faster than the rate of phosphoryl transfer ($k_{-2} > k_3$) and is in rapid exchange with the active site. By comparison, the large viscosity effect on k_{cat}/K_{ATP} implies that ATP dissociates from the enzyme slowly compared to the rate of phosphoryl transfer ($k_{-1} < k_3$). Given these results, $k_{cat}/K_{peptide}$ must be limited by the ratio of the phosphoryl transfer step and the dissociation constant for peptide (k_3/K_d) and k_{cat}/K_{ATP} must be limited solely by the rate constant for ATP association (k_1).

Isotope partitioning experiments have been applied previously to determine the exchange rates of ATP and Kemptide in the active site of bovine PKA at 0.5 and 10 mM free Mg^{2+} (*24*). These studies demonstrate that ATP dissociates slowly from the enzyme compared to the catalytic step at all magnesium levels, implying that k_{cat}/K_{ATP} is limited by the rate of nucleotide association. The viscosity data for recombinant mouse PKA agrees with these ATP studies at both low and high free Mg^{2+}. At low Mg^{2+}, however, the viscosity data indicate that Kemptide dissociates rapidly whereas isotope trapping suggests that Kemptide dissociates slowly. This discrepancy may be due to the choice of substrate in both experiments. The isotope exchange studies were performed with an acetylated Kemptide while our viscosity studies were performed with a peptide substrate possessing a free amino terminus. The K_m for acetyl Kemptide is approximately 10-fold lower than that for unmodified Kemptide (*8*, *24*) suggesting that both substrates may have different exchange properties in the active site. For example, when phosphoryl transfer is fast (i.e., $k_3 > k_4$), the K_m for Kemptide is either k_4/k_2 (when $k_3 > k_{-2}$) or K_dk_4/k_3 (when $k_{-2} > k_3$).

What is the Rate of Phosphoryl Transfer? To obtain direct information on the phosphoryl transfer step, we measured the phosphorylation of the peptide substrate prior to the accumulation of the steady-state species. As shown in Figure 3A, the production of phosphopeptide is biphasic at saturating Kemptide concentrations (200 μM). The slow, linear phase is ATP-dependent (Figure 3B) and provides values for K_{ATP} and k_{cat} that are similar to those measured using the coupled enzyme assay (Tables 1 and 3). This confirms that the linear phase in the quench flow experiment corresponds to the steady-state kinetic rate. The rapid burst in product at all ATP concentrations corresponds to a fitted rate constant of approximately 500 s^{-1}. This value, however, must be interpreted cautiously since the effective deadtime of the instrument is 2 ms and approximately 40% of the initial burst phase is complete at this fast rate constant (vide infra).

Previous kinetic analyses of PKA at 10 mM free magnesium showed that the observed burst rate constant, k_b, varies hyperbolically with the concentration of Kemptide (*1*) and can be fit to eq 3 when $k_{-2} > k_3$,

$$k_b = \frac{k_3[S]}{[S] + K_d} + k_4 \quad (6)$$

In this equation K_d is the dissociation constant for Kemptide from the ternary complex, E·ATP·S, and k_3 and k_4 are defined in Scheme 1. Although k_b is large at concentrations of Kemptide exceeding 50 μM, k_b is 150 s^{-1} at 10 μM Kemptide (Figure 4A), a rate constant that can be measured accurately in the rapid quench flow instrument. We can use eq 6, the value of k_4 obtained from viscosity measurements, and the dissociation constant for the competitive inhibitor, LRRAALG (Table 1), to estimate a value of 500 s^{-1} for k_3. Although an assumption in this treatment of the data is that the K_I for LRRAALG is similar to the K_d for Kemptide, we have shown in other studies with wild-type and mutant PKA's that K_d and K_I are very close in value (*1*, *25*−*27*). While we cannot measure directly a rate constant of 500 s^{-1} in our instrument, we assume that phosphoryl transfer is not less than this value since the amplitude of the burst phase at high ATP and Kemptide concentrations is close to 1 (Table 3). [2] Although the second magnesium ion in the active site of PKA is considered an inhibitory metal owing to its effect on turnover (Figure 1), this inhibitory ability does not extend to the phosphoryl transfer step since the rate constant for phosphoryl transfer appears to be equivalently large at 0.5 mM and 10 mM free Mg^{2+}.

A Conformational Change Precedes the Phosphoryl Transfer Step. Viscosity studies indicate that the association rate constant for ATP, k_1, limits k_{cat}/K_{ATP} (Scheme 2 and Table 2). Consequently, the pre-steady-state kinetic transients for ATP binding and phosphotransfer (Figure 5A) cannot be interpreted in the same manner as Kemptide binding (Figure 4A). Instead, we applied numerical integration using the kinetic simulation program KINSIM (*16*) and Scheme 3 to interpret the data in Figure 5.

Scheme 3 is similar to the kinetic mechanism in Scheme 2 except that k_1 is replaced with k_1' and k_{-1} is ignored since ATP is sticky (i.e., $k_{-1} < k_3$). For the kinetic simulations, we fixed initially the value of k_3 (500 s^{-1}) and varied k_1' and k_4 to get the best fit to the data. The two data sets in Figure 5A were best modeled when k_1' was set at 0.30 and 0.06 μM^{-1} s^{-1} at 0.2 and 3 mM ATP, respectively, and k_4 was set at 70 s^{-1}. By varying k_4, we could not find conditions where k_1' is invariant (data not shown). Also, we did not obtain significantly different values of k_1' and k_4 by increasing k_3 above 500 s^{-1} (data not shown).

The data sets at 1, 2, and 4 mM ATP (not shown in Figure 5A) were also modeled to obtain suitable values of k_1' (k_4 was best fit at 70 s^{-1}). The values of k_1'[ATP] that best fit the experimental data are shown plotted in Figure 5B as a function of ATP concentration. Although the values of k_1'-[ATP] are expected to respond linearly with the nucleotide concentration owing to the bimolecular nature of the reaction, there is no change in this term between 1 and 4 mM ATP. If the association of ATP and the attainment of the ternary complex, E·ATP·S, is limited purely by k_1 (0.24 μM^{-1} s^{-1}), as predicted by the viscosity studies, the observed rate for ATP binding would be faster than the rate for phosphoryl transfer above 2 mM ATP (Figure 5B). Since k_1'[ATP] remains constant at 170 s^{-1} above 1 mM ATP, a rate value well below our estimated phosphoryl transfer rate (500 s^{-1}),

Scheme 3

$$E{\bullet}S \xrightarrow{k_1'[ATP]} E{\bullet}ATP{\bullet}S \xrightarrow{k_3} E{\bullet}ADP{\bullet}P \xrightarrow{k_4}$$

we presume that the overall binding of ATP must limit the burst phase. This implies that an ATP-related conformational change step precedes the phosphoryl transfer step and effectively limits its value. To illustrate this phenomenon, we simulated the pre-steady-state kinetics for Kemptide phosphorylation assuming that ATP binding is limited only by the bimolecular association rate constant, k_1 (i.e., $k_1' = k_1 = 0.24\ \mu M^{-1}\ s^{-1}$). For this simulation, shown in Figure 5A using a dotted line, the value of k_4 is 50 s^{-1} which maintains the appropriate k_{cat} of 45 s^{-1}. The initial burst phase in this simulation is considerably faster and larger in the simulated data compared to the experimental data. While we have treated this conformational change as a component of k_1' in Scheme 3 in our simulations, it is not clear whether this step occurs before or after ATP binding and it is possible to satisfy the quench flow data with either scenario. We will address the reaction sequence in a later section. Nonetheless, this obligatory conformational change event precedes phosphoryl transfer, is ATP-linked, and limits the burst rate constant.

Are There Conformational Changes at High Free Magnesium? The evidence for an ATP-linked conformational change at physiological Mg^{2+} levels led us to speculate whether this step occurs at high free Mg^{2+}. The phosphorylation of Kemptide was monitored under identical conditions of ATP and Kemptide at 2 concentrations of free Mg^{2+} (0.5 and 10 mM) to see whether ATP binding limits the phosphoryl transfer step (Figure 6). At 0.5 mM free Mg^{2+}, a shallow, slow burst phase is observed, consistent with the data presented in Figure 5A. The line drawn through the data was generated from Scheme 3 using a kinetic simulation program and is consistent with a slow conformational change preceding the phosphoryl transfer step (Figure 5B). By comparison, the high values for α/[E] (0.9) and k_b (approximately 300 s^{-1}) at 10 mM free Mg^{2+} indicate that phosphoryl transfer is fast under high metal concentrations and is not impeded by a slower, prior conformational change step. While these data cannot exclude a conformational step at higher magnesium levels, the rate value for this step would greatly exceed 170 s^{-1}. Furthermore, owing to the low value of k_{cat} at 10 mM free Mg^{2+} (20 s^{-1}), such a conformational change step would not participate in limiting turnover.

Dissociation Constant for ATP. Since ATP dissociates slowly from the active site of PKA, no direct information regarding the dissociation constant of the nucleotide can be gathered from the viscosity studies. Likewise, no information can be obtained from pre-steady-state kinetic studies when ATP is the mixing ligand (Figure 5A). To determine the true affinity of ATP, we modeled the pre-steady-state kinetic transients under conditions of varied ATP pre-equilibration. Figure 7 displays the production of phosphopeptide as a function of time under conditions of 0.2 and 0.5 mM ATP and 0.2 mM Kemptide. The dotted lines drawn through the experimental data were obtained from kinetic simulations using Scheme 4, where k_1, K_d, k_3, and k_4 are set at 0.24 μM^{-1} s^{-1}, 40 μM, 500 s^{-1}, and 50 s^{-1}, respectively. The simulations begin with variable amounts of E and E·ATP based on a selected K_d for ATP (i.e., k_{-1}/k_1) and the initial concentration

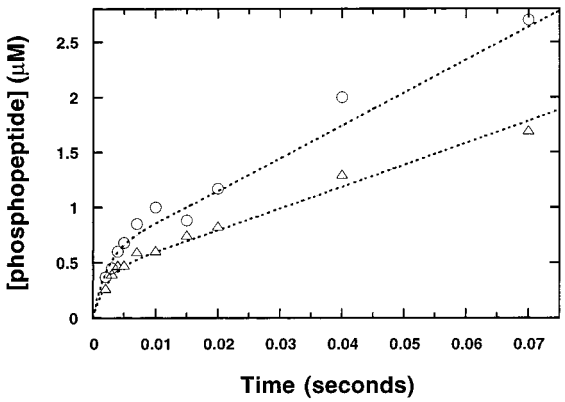

FIGURE 7: Phosphorylation of Kemptide using 0.2 (△) and 0.5 (○) mM ATP pre-equilibrated with PKA. C-subunit (final concentration: 3.2 μM) is pre-equilibrated with varying ATP and Mg^{2+} prior to starting the reaction with 200 μM Kemptide in 50 mM Mops (pH 7). The dotted lines drawn through the data were obtained from kinetic simulations using Scheme 4 (see text).

Scheme 4

$$E \underset{k_{-1}}{\overset{k_1[ATP]}{\rightleftharpoons}} E{\bullet}ATP \underset{K_d}{\overset{[S]}{\rightleftharpoons}} E{\bullet}ATP{\bullet}S \xrightarrow{k_3} E{\bullet}ADP{\bullet}P \xrightarrow{k_4}$$

of the nucleotide. The best simulations to the two data sets in Figure 7 arise when k_{-1} is approximately 50 s^{-1}, providing a K_d for ATP of 200 μM. In these simulations, we assume an ordered addition of ATP and Kemptide for simplicity but recognize that the substrate peptide binds the free enzyme upon mixing. In fact, isotope partitioning and detailed inhibitor studies indicate that ATP and substrate binding are random and nonsynergistic (*8*, *24*). We have shown in more complex simulations that the same K_d for ATP is obtained if the nucleotide and substrate bind independently (data not shown). In these simulations, we ignored the conformational change step that limits ATP binding since the low concentrations of ATP conceals this step (i.e., k_1[ATP] <170 s^{-1}). Nonetheless, this step is included by choosing a low value of k_4 (50 vs 70 s^{-1}). The kinetic mechanism in Scheme 4 is a simplification of a phosphoryl transfer mechanism that involves a conformational change associated with ATP binding. Accordingly, the value of 50 s^{-1} for k_{-1} may not represent a single step as indicated in Scheme 4 but may consist of a collection of rate constants associated with nucleotide binding and conformational changes. The simulations in Figure 7 demonstrate that K_{ATP} is close in value to the true dissociation constant for ATP. This equivalence, however, does not occur due to a slow phosphoryl transfer step but rather is a result of similar values for k_{-1} and k_4 [note that $K_d(ATP) = k_{-1}/k_1$ and $K_{ATP} = k_4/k_1$]. Finally, the similarity between K_{app} (Table 3) and K_{ATP} (Table 1) indicates that the ATP dependence on the burst amplitude in Figure 3B measures the fractional amount of enzyme-bound ATP (i.e., [E·ATP]/$[E]_o$).

Does the Conformational Change Precede ATP Association? While it is not uncommon for the association of ligands and enzymes to be accompanied by a unimolecular, conformational change step, the positioning of the latter step with respect to the bimolecular step is not easily surmised. In fact, a satisfactory solution to the kinetic data in Figure 5 can be obtained whether the conformational change precedes or occurs after the ATP association step. However, a consideration of the dissociation constant for ATP, the pre-steady-

Scheme 5

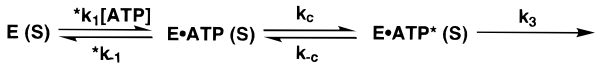

Scheme 6

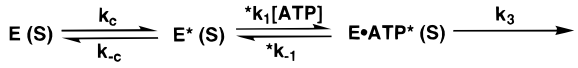

state kinetics and the exchange properties of the nucleotide in the active site favor only one of these mechanisms. To illustrate this point, consider the two mechanistic extremes for ATP binding in Schemes 5 and 6.

In these mechanisms the substrate is placed in parentheses to indicate that binding is rapid, does not present a large energetic barrier at high substrate concentrations, and may occur with any of these complexes, but phosphoryl transfer occurs only in the ternary complex. The bimolecular steps in both mechanisms are distinguished from those in Schemes 2−4 with a "starred" prefix. Under conditions of ATP pre-equilibration, S can bind rapidly to E·ATP or E·ATP*. In either mechanism ATP can bind to only one enzyme form, E(S) or E*(S).

In Scheme 5, the following conditions can be placed on the kinetic pathway on the basis of pre-steady-state kinetic and viscosometric experiments: $*k_{-1} < k_c > k_{-c} < k_3$. These conditions are based upon three observations: (1) The equilibrium constant for the conformational change ($K_{eq} = k_c/k_{-c}$) must be large to account for the large burst amplitude when the C-subunit, pre-equilibrated with ATP, is mixed with Kemptide. We place a lower limit of 10 for K_{eq} to account for the data in Table 3. (2) Since K_{eq} is large and the observed rate for the conformational change is slower than phosphoryl transfer (Figure 5), the rate constant of the phosphoryl transfer step must exceed the reverse rate constant for the conformational change step ($k_3 > k_{-c}$). (3) Owing to the large viscosity effect on k_{cat}/K_{ATP} (Table 2), ATP must be sticky ($k_{cat}/K_{ATP} = *k_1$) and the rate constant of the conformational change step must exceed the rate constant for ATP dissociation ($k_c > *k_{-1}$). Given the value of 170 s^{-1} for k_c, we place an upper limit of 20 s^{-1} for $*k_{-1}$. With these constraints, the dissociation constant for ATP in Scheme 5 is less than or equal to 10 μM [$K_d(ATP) = *k_{-1}/*k_1K_{eq}$]. Since this predicted K_d is, at least, 20-fold lower than the experimental value, Scheme 5 does not adequately depict the mechanism for ATP binding.

In Scheme 6, the following conditions can be placed on the kinetic pathway on the basis of pre-steady-state kinetic and viscosometric experiments: $k_c < k_{-c}$ and $k_3 < k_{-1}$. These conditions are based upon two observations: (1) The equilibrium constant for the conformational change ($K_{eq} = k_c/k_{-c}$) must be small to account for the small burst amplitude when the C-subunit is not pre-equilibrated with ATP. (2) Owing to the large viscosity effect on k_{cat}/K_{ATP} (Table 2), ATP must be sticky ($k_{cat}/K_{ATP} = *k_1K_{eq}$ if $K_{eq}<1$) and the rate constant of the phosphoryl transfer step must exceed the rate constant for ATP dissociation ($k_3 > *k_{-1}$). Given the estimated value of 500 s^{-1} for k_3, we place an upper limit of 50 s^{-1} for $*k_{-1}$. With these constraints, the dissociation constant for ATP in Scheme 6 is less than or equal to 210 μM [$K_d(ATP) = *k_{-1}/*k_1K_{eq}$]. Since this estimate range is within the experimental value of 200 μM, Scheme 6 satisfies the kinetic data and more closely represents the mechanism of ATP association.

Conclusions. PKA shows complex, magnesium-dependent steady-state rate behavior. Our data demonstrate that K_{ATP} at 0.5 mM free Mg^{2+} is equivalent to the K_d for ATP. Also, the 20-fold increase in K_{ATP} at 0.5 mM compared to 10 mM free Mg^{2+} is due to a proportional increase in the K_d value. Although occupancy of the second metal site improves ATP binding affinity, the observed increase in k_{cat}/K_{ATP} at high free Mg^{2+} is due mostly to improvements in the rate-limiting encounter of ATP with the active site. The observed association rate constant for ATP (k_1) is 5-fold higher at 10 versus 0.5 mM free Mg^{2+}. Kemptide exchanges rapidly with the active site at both 0.5 mM and 10 mM free Mg^{2+} but binds 4-fold more tightly under the former conditions. Overall, the data show that occupancy of the second metal site has the opposing effects of increasing ATP affinity and decreasing Kemptide affinity.

The rate of phosphoryl transfer is fast at both magnesium levels (approximately 500 s^{-1}) and does not significantly impact turnover. This is, indeed, a surprising result since the second metal makes a direct contact with the γ phosphate of ATP (*4*) and influences peptide affinity. The kinetic data show definitive evidence for a conformational change associated with ATP binding that precedes phosphoryl transfer and limits the burst phase at physiological metal. The rate constant of this structure change (170 s^{-1}) and the net rate constant for product release (70 s^{-1}) partially control k_{cat} (45 s^{-1}). We have shown previously that a conformational change partially limits turnover for a fluorescently labeled mutant of PKA (*11*) but have found no evidence for such a structural change in the wild-type enzyme at high magnesium (*12*). While the conformational step identified in the present study may still occur under high magnesium concentrations, its rate value must be significantly greater than 170 s^{-1} and would not participate in limiting k_{cat}. The data presented herein represent the first observation of an obligatory conformational change step in the phosphotransfer mechanism of wild-type PKA. We propose that this critical step supports a movement of several key catalytic residues essential for phosphoryl group transfer.

ACKNOWLEDGMENT

We would like to thank Siv Garrod and Dr. Susan S. Taylor for providing us with the inhibitor peptides, LRRAALG and LRRNALG. We also would like to thank Dr. John Hirai for technical assistance with the rapid quench flow experiments.

REFERENCES

1. Grant, B., and Adams, J. A. (1996) *Biochemistry 35*, 2022−2029.
2. Slice, L. W., and Taylor, S. S. (1989) *J. Biol. Chem. 264*, 20940−20946.
3. Madhusudan, Trafny, E. A., Xuong, N.-h., Adams, J. A., Ten Eyck, L. F., Taylor, S. S., and Sowadski, J. M. (1994) *Protein Sci. 3*, 176−187.
4. Zheng, J., Knighton, D. R., Ten Eyck, L. F., Karlsson, R., Xuong, N.-h., Taylor, S. S., and Sowadski, J. M. (1993) *Biochemistry 32*, 2154−2161.
5. Zheng, J., Trafny, E. A., Knighton, D. R., Xuong, N.-h., Taylor, S. S., Ten Eyck, L. F., and Sowadski, J. M. (1993) *Acta Crystallogr., Sect. D 49*, 362−365.

6. Knighton, D. R., Zheng, J., Ten Eyck, L. F., Ashford, V. A., Xuong, N.-h., Taylor, S. S., and Sowadski, J. M. (1991) *Science 253*, 407−414.
7. Romani, A., and Scarpa, A. (1992) *Arch. Biochem. Biophys. 298*, 1−12.
8. Cook, P. F., Neville, M. E., Vrana, K. E., Hartl, F. T., and Roskoski, J. R. (1982) *Biochemistry 21*, 5794−5799.
9. Sun, G., and Budde, R. J. A. (1997) *Biochemistry 36*, 2139−2146.
10. Saylor, P., Wang, C., Hirai, T. J., and Adams, J. A. (1998) *Biochemistry 37*, 12624−12630.
11. Lew, J., Taylor, S. S., and Adams, J. A. (1997) *Biochemistry 36*, 6717−6724.
12. Zhou, J., and Adams, J. A. (1997) *Biochemistry 36*, 15733−15738.
13. Martell, A. E., and Smith, R. M. (1977) *Critical Stability Constants*, Vol. 3, Plenum, New York.
14. Kemp, B. E., Graves, D. J., Benjamini, E., and Krebs, E. G. (1977) *J. Biol. Chem. 252*, 4888−4894.
15. Shoemaker, D. P., and Garland, C. W. (1962) *Experiments in Physical Chemistry*, 2nd ed., McGraw-Hill, New York.
16. Barshop, B. A., Wrenn, R. F., and Frieden, C. (1983) *Anal. Biochem. 130*, 134−145.
17. Adams, J. A., and Taylor, S. S. (1993) *J. Biol. Chem. 268*, 7747−7752.
18. Russo, A. A., Jeffrey, P. D., and Pavletich, N. P. (1996) *Nat. Struct. Biol. 3*, 696−700.
19. Jeffrey, P. D., Russo, A. A., Polyak, K., Gibbs, E., Hurwitz, J., Massague, J., and Pavletich, N. P. (1995) *Nature 376*, 313−320.
20. Hubbard, S. R., Wei, L., Ellis, L., and Hendrickson, W. A. (1994) *Nature 372*, 746−754.
21. Hubbard, S. R. (1997) *EMBO J. 16*, 5572−5581.
22. Zhang, F., Strand, A., Robbins, D., Cobbs, M. H., and Goldsmith, E. J. (1994) *Nature 367*, 704−711.
23. Canagarajah, B. J., Khokhlatchev, A., Cobb, M. H., and Goldsmith, E. J. (1997) *Cell 90*, 859−869.
24. Kong, C.-T., and Cook, P. F. (1988) *Biochemistry 27*, 4795−4799.
25. Grant, B. D., Tsigelny, I., Adams, J. A., and Taylor, S. S. (1996) *Protein Sci. 5*, 1316−1324.
26. Grant, B. D., Hemmer, W., Tsigelny, I., Adams, J. A., and Taylor, S. S. (1998) *Biochemistry 37*, 7708−7715.
27. Adams, J. A., McGlone, M. L., Gibson, R., and Taylor, S. S. (1995) *Biochemistry 34*, 2447−2454.
28. Adams, J. A., and Taylor, S. S. (1992) *Biochemistry 31*, 8516−8522.

BI982768Q